RESEARCH ARTICLE

Dynamic Response Analysis of Asynchronous Deicing of Quad Bundle Conductor Spacer System During DC Ice Melting

ZHU HE[1], (Fellow, IEEE), TANG WENPENG[1], ZHANG RENQI[2], WANG WEIQI[1], AND LIAO HANLIANG[1]

[1]School of Civil Engineering and Architecture, Northeast Electric Power University, Jilin City, Jilin 132012, China
[2]Guizhou Electric Power Test Research Institute, Guiyang 550002, China

Corresponding author: Zhu He (Zhuhe1215@163.com)

ABSTRACT In order to study the melting and falling off of the iced conductor under DC ice melting process by considering a lgj-400 / 50 transmission conductor as a research object, Ansys LS-DYNA model is used for simulating the response of materials under short periods of high-intensity loads and a nonlinear structural dynamics model is used to establish the finite element model of split conductor system in the actual process. In the process of finite element analysis, solid45 element is used to model the conductor layer by layer. During the calculation process, the life and death element method is used to transform its element stiffness matrix to near zero icing element for accurately simulating the actual situation during ice melting. Currently, the research on the deicing of the split conductor mostly equates the split conductor to a single conductor for calculation. In the actual ice melting operation, the split conductor system has a phenomenon of asynchronous deicing, so it is necessary to analyze the deicing of different sub-conductors. The results show that the jump height of the deicing conductor under DC deicing is smaller than that of the normal deicing. The jump height and tension of conductor deicing decrease with an increase in the deicing current. When the sub-conductors of the four-bundle conductor spacer system are not deiced synchronously, the two sub-conductors on the diagonal and two sub-conductors below are deiced, the split conductor system is relatively stable. When the sub-conductors under other working conditions are not deiced synchronously, the four-bundle conductor spacer system has lateral swing, resulting in torsional risk, which causes conductor wear and strand breaking accidents.

INDEX TERMS Asynchronous deicing, DC melting ice, dynamic response, split conductor spacer system, sub-conductor.

I. INTRODUCTION

During winters in southern China, low temperature, rain, and snow seriously impact the power grid equipment leading to power outages, thus affecting the daily life of people. The icing formed on the transmission lines during the winter season has become one of the most serious disasters that threaten the safe operations of China's power grid [1], [2].

The associate editor coordinating the review of this manuscript and approving it for publication was Ali Raza.

At present, more than 30 deicing methods have been adopted to address this problem. However, most of these methods cannot be applied to the transmission lines due to the lack of practicality and high cost. The production of heat based on DC melting is the most effective deicing method. As compared with other de-icing methods, this method is simple to implement, and has less impact on the power grid in terms of security [3], [4], [5], [6].

There are various works presented in literature that affect the dynamic response of transmission wire icing shedding.

Wang et al. [7] and [8] conducted an experimental study on the dynamic tension in the vibration process of transmission wire deicing. The authors analyzed the dynamic tension variation characteristics of the wire under different deicing speeds and different deicing modes. Huang Xinbo et al. [9] analyzed the tension imbalance in the wire during the deicing process by establishing a calculation model of multi-stage wire under different conditions of deicing method and icing thickness. There are various works [7], [9] that have studied the change in tension change of the ice-covered wires during deicing, and analyzed the dynamic tension change characteristics of the wire under different deicing methods.

Li et al. [10] measured wire tension and mid-span jump height under different icing thickness and speed of wind by establishing a single wire test model and using equivalent mass block instead of icing simulation. Kunpeng Ji et al. [11] established a new type of ice-covered wire model by using a 3D beam unit in ADINA software. The authors compared and analyzed the deicing test data acquired from an outdoor distance of 100m during winter for verifying the accuracy of the proposed model. Jamaleddine et al. [12] conducted a simulation test on the scale model by using a two-stage transmission wire with a length of 3.22m in the laboratory, and simulated the ice-covered shedding of the wire by controlling the shedding mode of the electromagnet. The ADINA simulation analysis software was also used for performing numerical simulations and analyzing the jump height of the wire after deicing. In [10], [11], and [12], different methods are used to simulate icing for performing experiments, and the dynamic response of the wire after ice shedding was calculated.

Wu Chuan [13] established models of different conductors based on finite element simulation and analyzed the jumping height of conductors under different icing thickness and spacing. Based on ADINA finite element simulation, Wu Tianbao [14] analyzed the influence of jump height of ice-covered wires after deicing under different conditions, such as icing thickness, deicing position, and wire length. Yan Zhitao [15] studied the influence of height on wire jumping in finite element simulation by using 3-DOF suspension cable element and life-or-death element method to simulate ice shedding. Shan Gao [16] established the wine cup tower wire system and calculated the deicing jump height of the wire in different deicing modes by considering the initial tension. The finite element analysis software was used in [13], [14], [15], and [16] to analyze the change in the jump height of ice-covered wires with respect to time under different deicing methods. Shen Guohui [17] calculated the split wire equivalent to a single wire and proposed the equivalent calculation method when the split wire and the single wire are covered with ice and fall off. Dong Yongxing [18] analyzed the jump height, wire tension and torsion angle of the split wire system for asynchronous deicing between the neutron wires in the six-split wire-spacer system. Gui Zaohuang [19] and [20] compared and verified the scale test of wire deicing based on the numerical simulations, improved the calculation

formula of maximum deicing jump height, and simulated the torsional characteristics of four-split wires under different torques. The authors in [17], [18], [19], and [20] studied the deicing jump height and torsion angle of the split wire system.

All of the aforementioned works focused on the dynamic response of the wire during deicing and analyzed the influence of different types of wires, icing thickness, and spacing. Please note that during the process of wire ice shedding, the influence of melting current is not considered. For split conductor systems, various works equate the conductor wire into a single wire calculation during the icing shedding process, ignore the phenomenon of unsynchronized de-icing between each sub-wire, and calculate the overall dynamic response of the split wire system during the unsynchronized de-icing. However, the de-icing jump and lateral swing of each sub-conductor under the constraint of the spacer rod are ignored. In actual ice-melting process, the asynchronous deicing phenomenon exists in the split wire system. The lateral swing of the split wire system is restrained by the spacer bar during deicing, which leads to torsion of the split wire system. Therefore, based on the four-split wire that is commonly used in the power lines in southwest China, ANSYS finite element software is used to calculate the four-split wire-spacer system. Moreover, we also analyze the displacement and torsion angle of the wires under deicing of different sub-wires and study the dynamic response of the asynchronous deicing of each sub-wire during the DC melting of the four-split wire system.

II. VIBRATION EQUATION OF DC MELTING ICE IN FOUR - SPLIT WIRE - SPACER SYSTEM

During the process of DC melting, the joule heat of the four-split wire is generated constantly due to the action of the melting current. As a result, the ice continuously keeps melting. The load on the wire mainly comprises the ice load. For a dynamic wire system structure, the ice load and displacement are functions of time t.

Based on D 'Alembel principle, the concentrated mass method is adopted to balance the wire between N concentrated mass points. Each wire contains three degrees of freedom, i.e., vertical, horizontal, and torsion. The dynamic equation of DC melting process in the transmission line is established [21], and is mathematically expressed as follows:

$$[M]\ddot{u} + [C]\dot{u} + [K]\Delta u = F(t) \tag{1}$$

where, $\ddot{u}$, $\dot{u}$, and Δu denote the acceleration, velocity, and displacement increment vectors of the system, respectively. $[M]$ represents the mass matrix, $[C]$ represents the damping matrix, and $[K]$ represents the stiffness matrix. Please note that the stiffness matrix $[K]$ contains the stiffness coefficient of each mass point, which is obtained by combining each point. That is, if a unit displacement or angle is generated on the j-th degree of freedom, the force or moment needs to be applied on the i-th degree of freedom. In this work, we propose to use the solid element simulation model for applying a unit load at each mass point and solve the flexibility

coefficient matrix in combination with the corresponding displacement. The stiffness coefficient matrix is obtained by taking the inverse of matrix $F(t)$ in (1) denotes the dynamic ice load, which changes with the shedding of ice during the process of DC melting, as shown in (2):

$$F(t) = [\rho_{con} V_{con} + \rho_{ice} V_{ice}(t)] g \qquad (2)$$

where, g denotes gravitational acceleration, i.e., 9.8m/s². ρ_{con} represents the density of the conductor, ρ_{ice} represents the density of the ice. $V_{con}(t)$ represents the volume of the conductor, V_{ice} represents the volume of the ice which changes with the time of DC melting.

III. CALCULATION CONDITIONS OF DC MELTING ICE IN FOUR-SPLIT WIRE SPACER SYSTEM

According to the actual experience in the process of DC melting, there is an asynchronous deicing phenomenon for the split wire. Please note that the deicing time of the neutron wire of the split wire is inconsistent. Therefore, all the wires cannot be covered with ice and shed it at the same time during the actual melting process. In this work, considering four split wire rod system DC melting ice interval, different sub-conductor ice coating fall off when jumping analysis, reference Xing Liang jiang [22] xue feng mountain in Hunan DC thawing experiment, observation records conductor DC most conductor ice melting ice in a relatively short time falls off phenomenon, to understand different child lead split off ice lead system dynamic response of each wire. The sub-wires are calculated according to the deicing rate of 100%.

In finite element modeling, the transmission line and deicing parameters are determined based on the actual operation parameters of China southern power grid. The transmission wire spacing is set to 200m, and the wire type is LGJ-400/50. The parameters of the wire are shown in TABLE 1.

TABLE 1. The structural characteristics of LGJ-400/50 conductor.

Wire parameters	Wire parameters calculation value
Area (mm²)	451.55
Outside diameter (mm)	27.63
Pulling force (kN)	123.4
Quality (kg/km)	1511
Modulus of elasticity (N/mm²)	69000
Coefficient of thermal expansion (°C⁻¹)	19.3×10⁻⁶

In this work, 20mm rime icing condition is considered, which is common during the winter season in southwest China. For 20mm icing, the critical melting current of LGJ-400/50 wire is calculated based on the technical specification of the DC melting system design (DL/T5511-2016) [23]. Within the critical current range, according to the DC ice-melting operations of China southern power grid, the ice-melting time corresponding to 1000A ice-melting current is calculated. TABLE 2 presents the computation results.

The number of pairs of sub-wires in the four-split wire-spacer system is equal to the number of the sub-conductors,

and the dynamic response of deicing of the split wire system under different working conditions, such as deicing of single conductor, deicing of two sub-conductors, deicing of three sub-conductors, and deicing of four sub-conductors, are discussed. Fig. 1 presents the specific numbering and naming convention of sub-wires.
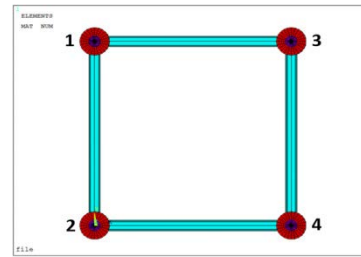

FIGURE 1. Diagram of the naming of each sub-conductor.

TABLE 2. The DC melting process parameters.

DC melting parameters	Calculated value
Equivalent ice conduction thermal resistance $(°C \cdot cm/W)$	0.081
Convection and radiation equivalent thermal resistance $(°C \cdot cm/W)$	0.099
Minimum melting current (A)	731.28
Maximum melting current (A)	1385.49
Actual melting current melting time (min)	83.6

IV. FINITE ELEMENT SIMULATION OF FOUR BUNDLE CONDUCTOR SPACER SYSTEM

A. FINITE ELEMENT MODEL OF FOUR BUNDLE CONDUCTOR SPACER SYSTEM

The authors in [24] discuss that for the transmission line system, the natural frequency of the transmission tower is much larger as compared to natural frequency of the transmission conductor. It is well-known that the coupling effect of the transmission line tower line system has a little influence on the deicing dynamic response of the transmission conductor and can be ignored.
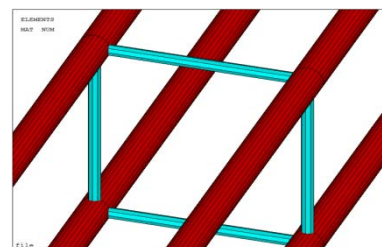

FIGURE 2. The finite element model of quad bundle conductor spacer system.

The modeling is closer to actual engineering conditions that are achieved by layering modeling between steel core,
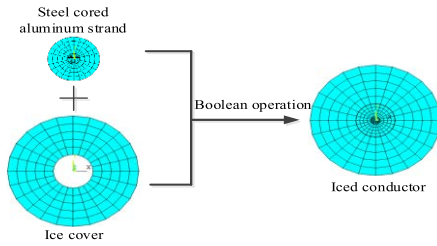
FIGURE 3. The finite element model of iced conductor.

aluminum wire, and ice layer. The layered modeling method is shown in Fig. 4. The inner layer represents the steel core, the middle layer denotes the aluminum wire, and the outermost layer represents the ice layer. Please note that all the grid cells in Fig. 4 are hexahedral, highly symmetrical, uniformly distributed as a whole, and orderly, which significantly improves the calculation speed and accuracy. The positions at both ends of the split wire system are considered suspension points, and the boundary conditions are imposed on each child wire node at both ends of the split wire system.
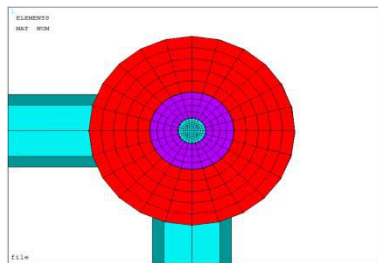

FIGURE 4. The grid division diagram of quad bundle conductor spacer system.

B. ACCURACY VERIFICATION OF FINITE ELEMENT MODEL
In order to verify the accuracy of the finite element model, it is necessary to analyze and compare the results of previous wires under DC melting. However, it is difficult to simulate the actual conditions of DC melting, so there are few experimental data samples of the dynamic response of DC melting wires at present. The results of author's test are compared with Meng's [17] test results of deicing dynamic characteristics of transmission wires with equal proportion of 235m pitch established in Wuhan State Grid Research Center. In this test, the ice weight was calculated based on the equivalent gravity method. The ice weight was equal to the actual sandbag weight. In addition, the hanging heavy steel rope was controlled by the electric cutter for simulating the ice falling off.

B-3 condition in Meng [17] test is selected for verification. The data comparison is shown in Fig. 6. In the test, the LGJ-630/45 steel-core aluminum stranded wire with a gear distance of 235m is covered with ice thickness of 15mm, and a single conductor is completely de-iced. A completely consistent calculation model is established according to B-3 working conditions in the finite element software. Three

degrees of freedom constraints are imposed on both ends of the wire, and the ice is attached to the wire by Boolean operation. Changing its element stiffness matrix to near zero ice-covered unit simulates ice-covered shedding. During the computation process, the wires are divided into 100 units on average, and the calculation time step is 0.05s. According to Rayleigh damping hypothesis, the damping matrix is a linear combination of mass matrix and stiffness matrix [16], as shown in (3).

$$[C] = \alpha [M] + \beta [K] \qquad (3)$$

where, α is the mass damping coefficient and β is the stiffness damping coefficient. These coefficients can be obtained by using (4) and (5), respectively.

$$\alpha = \frac{2\omega_i\omega_j(\xi_i\omega_j - \xi_j\omega_i)}{\omega_j^2 - \omega_i^2} \qquad (4)$$

$$\beta = \frac{2(\xi_j\omega_j - \xi_i\omega_i)}{\omega_j^2 - \omega_i^2} \qquad (5)$$

In (4) and (5), ω_i, ω_j represent the vibration frequency of the i-th and j-th order of the wire, respectively, which is calculated and obtained by using the ANSYS finite element software, ξ_i, ξ_j represent the damping ratio of the vibration mode of the i-th order and j-th order of the wire, and the value of the damping ratio of the ice-covered wire is 10% of the critical damping [26].
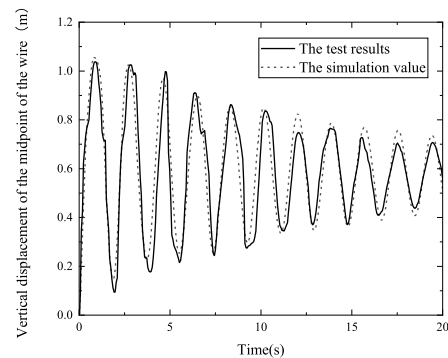

FIGURE 5. A comparison between finite element data and test data.

Fig. 5 shows that solid45 element modeling is used to simulate the ice falling off by birth and death element method in this work. The calculation model is in good agreement with the deicing test results conducted by Meng. Additionally, the conductor deicing jump height and trend are consistent, which indicates the accuracy of this method and lays a foundation for the following analysis.

C. FORM FINDING ANALYSIS OF ICED CONDUCTOR
First, we set the element type and material properties. Then, a large initial strain value is applied to the solid element, a small elastic modulus is set, and the self-weight load is applied. This method saves time and achieves high precision. At the same time, based on the form finding analysis method,

taking the corresponding relationship between horizontal tension and sag as the convergence condition, the initial deformation of iced conductor under self-weight and icing load is obtained. After the form finding, we restart the analysis, restore the actual parameters of the iced conductor, and set the actual strain of the material. The data after form finding of iced conductor is extracted by using the ANSYS finite element software. The theoretical value is calculated based on the catenary state equation [29] and compared with the theoretical calculation value of the conductor. The calculated data is shown in TABLE 3.

TABLE 3. A comparison and analysis of conductor shape finding data.

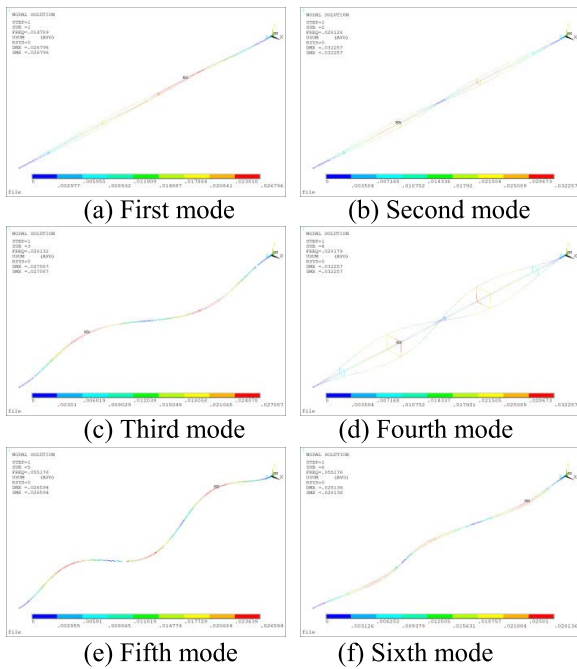|	Theoretical value	Simulation value	Error rate
Error rate (m)	3.636	3.6938	1.58%
tension (N)	56180	57647	2.61%
Y Directional support reaction (N)	32976	33390	1.26%

(a) First mode
(b) Second mode
(c) Third mode
(d) Fourth mode
(e) Fifth mode
(f) Sixth mode

FIGURE 6. The quad bundle conductor spacer system with different vibration modes.

D. MODAL ANALYSIS OF ICED CONDUCTOR UNDER PRESTRESS

There is prestress in the initial linear state of the iced conductor. Three degrees of freedom constraints are imposed on both ends of the split conductor system. The modal analysis is performed, and the frequency of the iced conductor is obtained, which shows the speed of the structural stiffness and deformation. Fig. 6 shows the first six vibration modes of the four-bundle conductor spacer system.

TABLE 4. The description of the sixth mode natural frequency and mode of the conductor.

Mode order	frequency (Hz) value	Vibration mode description value
1	0.092928	Y swing
2	0.176746	Y swing
3	0.176809	X-direction swing
4	0.177062	Y swing
5	0.346643	X-direction swing
6	0.347209	Y swing

According to the vibration theory, the lower order modes play a major role in the structural vibration process. On the other hand, the higher order modes have a little impact on the dynamic response and fast attenuation speed. Therefore, only the lower order frequency modes are considered for analysis. The finite element analysis data are invoked. TABLE 4 shows each order frequency and main vibration modes of the four-bundle conductor spacer system.

V. RESPONSE ANALYSIS OF FOUR BUNDLE CONDUCTOR SPACER SYSTEM ICING AND FALLING OFF

According to the calculation results presented in TABLE 2 combined with the ice melting experience in the actual operation of China southern power grid, in the finite element calculation process, for the DC ice melting of lgj-400 / 50 conductors, the ice melting current of single conductor will be 1000A for ice melting. In addition, the four-bundle conductors are four times the ice melting current of single conductor for ice melting. The life and death element method is used to change its element stiffness matrix to near zero icing element for simulating the ice falling off. The research parameters include four sub-conductors deicing at the same time, including single sub-conductor deicing, two sub-conductors deicing, and three sub-conductors deicing in the four-bundle conductor spacer system.

A. ANALYSIS OF SIMULTANEOUS DEICING OF FOUR SUB-CONDUCTORS

The dynamic response of four sub-conductors under simultaneous deicing is analyzed in order to effectively understand the dynamic response of the conductor deicing under the action of ice melting current. Considering that there is no ice melting current in the natural state, the actual ice melting current of the power grid under this icing condition is 1000A and the maximum ice melting current calculated in the regulations is 1350A. The deicing jump height of the four sub-conductors is calculated. Since the displacements of each sub-conductor are same and have no influence on each other when the four sub-conductors are deicing synchronously, the deicing jump height at the midpoint of the sub-conductor with the same number is selected. Fig. 7 presents the displacement time history curve.
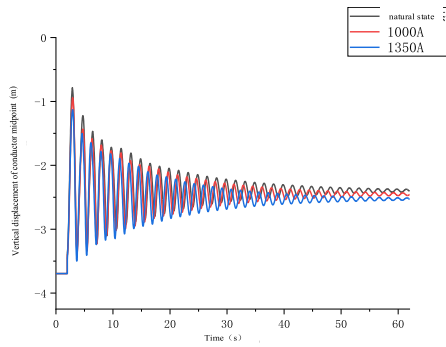
FIGURE 7. The time-history curve of vertical displacement of midpoint of conductor under different melting currents.

TABLE 5 shows the maximum jump height displacement and stable position height after deicing of four sub-conductors under different ice melting currents.

TABLE 5. The deicing jump values of conductors under different working conditions.

Deicing condition	Maximum jumping height of conductor (m)	Stable position height (m)
natural state	2.909	2.406
1000A	2.739	2.457
1350A	2.561	2.531

According to Fig. 7 and TABLE 5, under the influence of the same icing thickness, the jump height of conductor icing falling off decreases with an increase in the ice melting current. At the same time, the greater the ice melting current, the lower is the displacement of stable position after the conductor icing falls off. In order to effectively analyze the occurrence of this phenomenon, we extract the conductor tension value at the midpoint of sub-conductor with the same number when icing falls off. TABLE 6 presents the conductor tension.

TABLE 6 shows that under the action of different ice melting currents, the horizontal tension of the conductor decreases with an increase in the ice melting current. Under the action of the ice melting current, the structure of the conductor changes, and the wire length of the conductor becomes longer with an increase in the ice melting current, which leads to the reduction of displacement in the stable position after the ice coating falls off. At the same time, the greater the ice melting current, the lower is the jump height after the ice coating falls off.

TABLE 6. The midpoint tension values of conductors under different working conditions.

Deicing condition	Conductor tension (N)
natural state	57336
1000A	51610
1350A	49527

B. DEICING OF SINGLE SUB-CONDUCTOR

When analyzing the influence of a single sub-conductor deicing, due to the spacer system of four-bundle conductor being a symmetrical structure, No. 2 sub-conductor is selected for deicing, and the other three sub-conductors are not deiced for research and analysis.
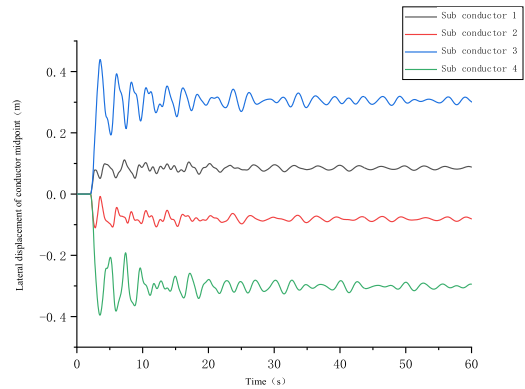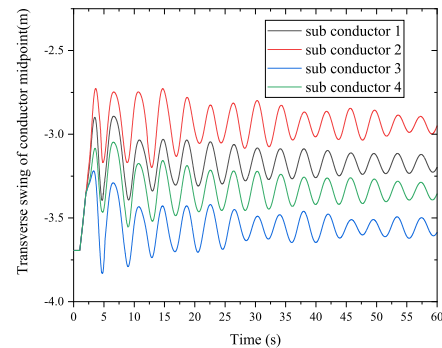

FIGURE 8. A lateral swing displacement time history of midpoint of each sub-conductor during the deicing of single sub-conductor.

For the lateral swing displacement of the conductor, the lateral swing of each sub-conductor presents a diagonal symmetrical trend. The lateral swing of No. 2 sub-conductor deicing is small, which is basically consistent with that of No. 3 sub-conductor without deicing on the diagonal. The lateral swing of No. 1 sub-conductor and No. 4 sub-conductor without deicing is large, and the maximum lateral swing displacement reaches 0.3 m.

Fig. 9 shows the torsional angle time history of the four-bundle conductor spacer system when a single sub-conductor is deiced. The results show that the maximum torsional angle reaches 13.6 °. When the deicing is completed, the overall torsional angle of the four-bundle conductor spacer system is 9.8 °.

C. ANALYSIS OF SIMULTANEOUS DEICING OF TWO SUB-CONDUCTORS

When analyzing the deicing of two sub-conductors, there are three deicing modes, namely diagonal two sub-conductors deicing, upper two sub-conductors deicing, and lower two sub-conductors deicing.
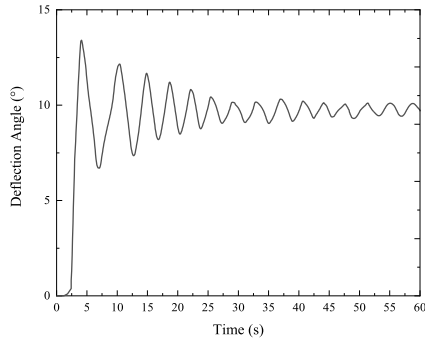
FIGURE 9. Torsional angle time history of split conductor system during deicing of single sub-conductor.

1) ANALYSIS OF SYNCHRONOUS DEICING OF DIAGONAL SUB-CONDUCTOR

No. 1 and No. 4 sub-conductors on the same diagonal are selected for deicing. When the two sub-conductors on the diagonal are deiced synchronously, the different sub-conductors of the four-bundle conductor spacer system are analyzed.
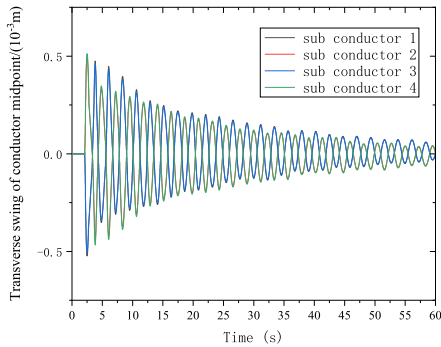

FIGURE 10. A lateral swing displacement time history of the midpoint of each sub-conductor during the deicing of diagonal sub-conductor.
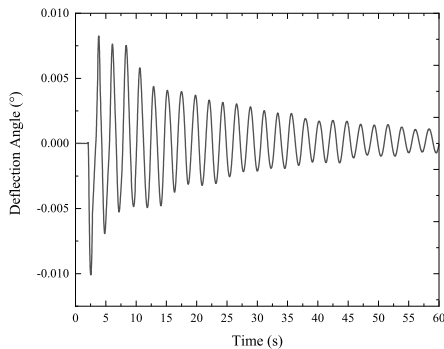

FIGURE 11. A torsional angle history of split conductor system during the deicing of diagonal sub-conductor.

The results presented in Fig. 10, and Fig. 11 show that when the diagonal sub-conductor is covered with ice and falls off at the same time, the displacement of the lateral swing of No. 1 and No. 4 sub-conductors basically show a symmetrical trend, and the displacement trend of the lateral swing of No. 2 and No. 3 conductors, which are not deiced

on the same diagonal, is the same. The displacement of the maximum lateral swing is only 5×10^{-4} m. The vertical jump height displacements of deicing No. 1 and No. 4 conductors have the same vibration trend as that of non-deicing conductors. The deflection angle of split conductor system is small, and the sub-conductor presents synchronous vibration jump phenomenon.

2) ANALYSIS OF SIMULTANEOUS DEICING OF TWO SUB-CONDUCTORS ON THE SAME SIDE

No. 3 and No. 4 sub-conductors on the same side are selected for deicing. When the two sub-conductors on the same side are deiced synchronously, the different sub-conductors of the four-bundle conductor spacer system are analyzed.
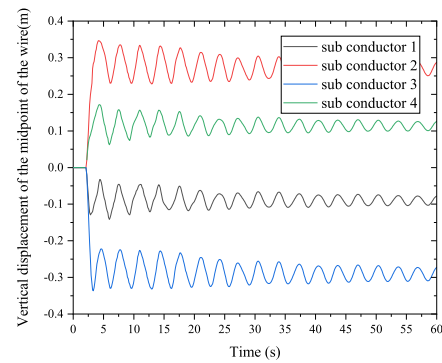

FIGURE 12. A lateral swing displacement time history of midpoint of each sub-conductor during the deicing of same side sub-conductor.
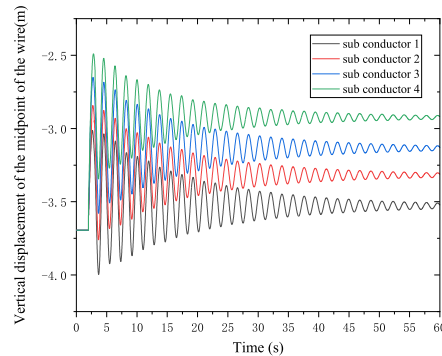

FIGURE 13. Time history of vertical jump displacement of midpoint of each sub-conductor during the deicing of same side sub-conductor.

The results presented in Fig. 12, Fig. 13, and Fig. 14 show that when No. 3 and No. 4 sub-conductors on the same side are deiced, the displacement of the lateral swing is smaller than that of No. 1 and No. 2 sub-conductors without deicing. Moreover, the displacement of the vertical jump is larger than that of No. 1 and No. 2 sub-conductors without deicing and the maximum torsion angle of split conductor system reaches 16.3 °. When the sub-conductor on the same side is deicing, the weight on one side of the split conductor system decreases, and the split conductor system is twisted to the deicing side as a whole under the constraint of the spacer.
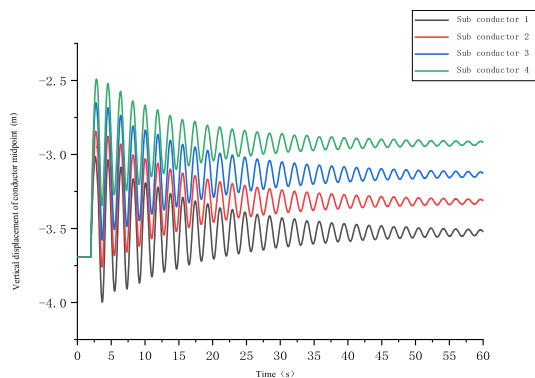
FIGURE 14. A torsional angle time history of split conductor system during deicing of the same side sub-conductor.

3) ANALYSIS OF SYNCHRONOUS DEICING OF TWO SUB-CONDUCTORS UNDER

Two sub-conductors, i.e., No. 2 and No. 4 sub-conductors, are selected for deicing in the split conductor system and different sub-conductors of the four split conductor spacer system are analyzed.
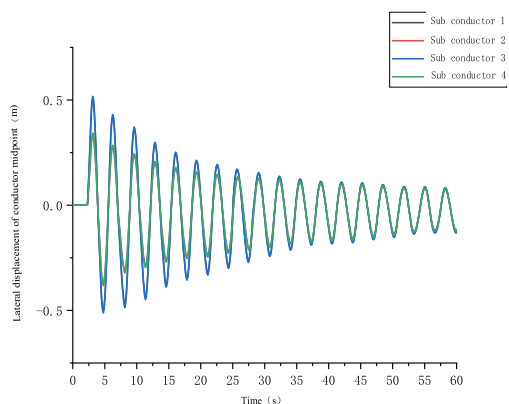

FIGURE 15. A lateral swing displacement time history of midpoint of each sub-conductor during the deicing of the lower sub-conductor.
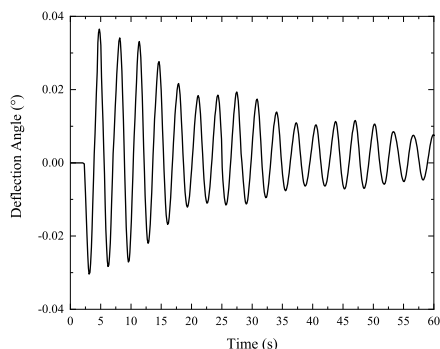

FIGURE 16. A torsional angle time history of split conductor system during the deicing of lower sub-conductor.

The results presented in Fig. 15, and Fig. 16 show that when No. 2 and No. 4 sub-conductors under the split conductor system are deiced at the same time, the lateral swing amplitude of the four sub-conductors is small, and the displacement is only 5×10^{-4}m. The vertical jump trend of the

four sub-conductors is consistent, and No. 3 sub-conductor on the lower side of the split conductor system has a large deicing jump height. When the lower two sub-conductors are deiced synchronously, the maximum torsional angle of the four-bundle conductor spacer system is 0.038 °, the torsional angle is small, and the four-bundle conductor spacer system tends to be stable.

D. ANALYSIS OF SYNCHRONOUS DEICING OF THREE SUB-CONDUCTORS

The deicing of No. 1, 3, and 4 sub-conductors is studied, and the different sub-conductors of the four-bundle conductor spacer system are analyzed.

The results presented in Fig. 17, Fig. 18, and Fig. 19 show that the displacement of lateral swing of No. 2 sub-conductor without deicing is larger by 0.17m as compared to the other three deicing conductors. The lateral swing of split conductor system is constrained by the action of spacer, and the lateral swing between sub-conductors on the diagonal is symmetrical. For the deicing jump height of the conductor, the displacement of deicing jump height of No. 2 sub-conductor without deicing is the smallest, and the displacement of the deicing jump height of No. 4 deicing conductor is the largest under the four-bundle conductor spacer system. When the three sub-conductors are deiced synchronously, the maximum torsion of the four-bundle conductor spacer system reaches 12.8 °. When the deicing is completed, the overall torsion of the four-bundle conductor spacer system is 8.2 °.
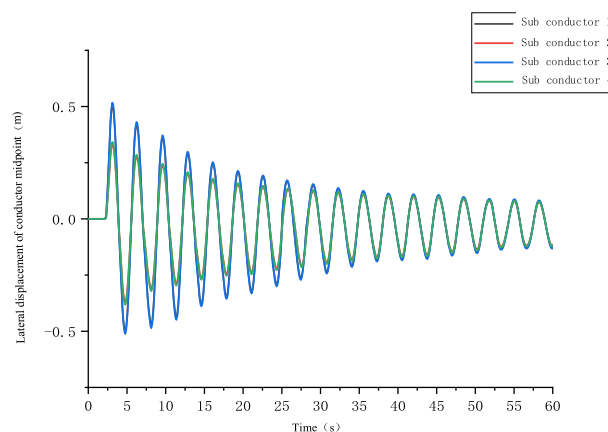

FIGURE 17. The lateral swing displacement time history of the midpoint of each sub-conductor during the deicing of three sub-conductors.

E. ANALYSIS OF CALCULATION RESULTS

The calculated results are compared with the theoretical expression of maximum height of deicing jump. Currently, the expression for calculating the maximum height of deicing jump in China's transmission line design [27] adopts the calculation method of the former Soviet Union, which is mathematically expressed as:

$$H = m\left(2 - l/1000\right)\Delta f \qquad (6)$$

TABLE 7. A comparison of maximum height of deicing jump in split conductor system.

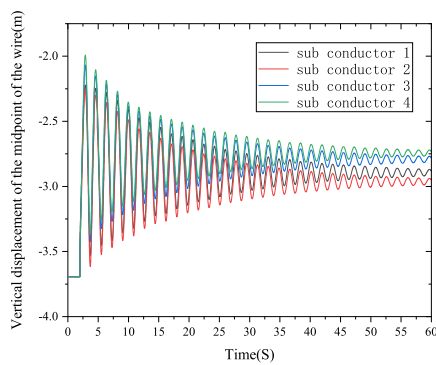| Calculation condition	Finite element calculation (m)	Procedure calculation (m)	Simplified formula calculation (m)
Diagonal sub-conductor deicing	1.056	1.025	1.036
deicing of lower sub-conductor	1.047	1.008	1.020
Calculation condition	Finite element calculation (m)	Procedure calculation (m)	Simplified formula calculation (m)

FIGURE 18. The vertical jump displacement time history of the midpoints of each sub-conductor during the deicing of three sub-conductors.
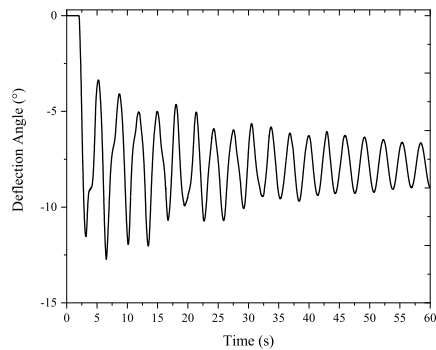

FIGURE 19. The torsional angle time history of split conductor system during the deicing of three sub-conductors.

where, l is span, Δf is the sag difference of iced conductor before and after deicing, and m is the constant introduced by considering the conductor deicing condition, which is taken as 1.0 when the whole gear is completely deiced.

The authors in [28] use linear regression to fit the calculation results obtained using the numerical simulations and summarize the simplified formula for calculating the deicing jump height of a conductor under short span, as shown in (7).

$$H = 1.82\Delta f \qquad (7)$$

According to the (4-1) and (4-2), as compared with the finite element calculation results presented in this work, the working conditions of diagonal sub-conductor deicing and lower sub-conductor deicing under the stable state of split conductor system are analyzed. The comparison of results is shown in TABLE 7.

The results presented in TABLE 7 show that under the conditions of diagonal sub-conductor deicing and lower sub-conductor deicing during asynchronous deicing of four-bundle conductor system, the maximum jump height calculated based on the finite element method in this work is close to the results of regulations and simplified theoretical formula. The error rate in the computed values is within 4%.

VI. CONCLUSION

In this work, the ls-dyna preppost module in ANSYS finite element software is used for performing nonlinear structural dynamics analysis. Considering an actual conductor, in this work, the conductor is modeled in layers, the shape finding analysis of iced conductor is performed, the ice melting current is applied, and the ice falling off is simulated by the life and death element method. As compared with the data presented in the existing literature, the reliability of this method is verified, and the following conclusions are drawn:

(1) For solid element conductor form finding analysis performed based on the form finding analysis method, the iterative calculation is carried out with the corresponding relationship between the horizontal tension and sag as the convergence condition. Then, it is compared with the theoretical calculation results of the string chain state equation. The error rate between the calculated value and the theoretical value is less than 3%.

(2) According to the relevant regulations, the critical minimum ice melting current and maximum ice melting current of the conductor are calculated. It is analyzed that under the action of ice melting current, the jumping height of the conductor deicing decreases with an increase in the ice melting current, and the stable position of conductor deicing increases with an increase in the ice melting current. These influencing rules provide relevant operation basis for line ice melting operation in practical engineering.

(3) When the quad bundle conductor spacer system is not de-iced synchronously, the two sub-conductors of the diagonal are synchronously de-iced, and the two sub-conductors on the lower side are synchronously de-iced. The lateral swing amplitude displacement of the conductor is small, and the vertical jump height is consistent. The overall trend of deicing the bundle conductor system is stable. During the actual ice melting operation of the split conductor, it is recommended to select the diagonal sub-conductor and the lower sub-conductor to melt the ice synchronously to avoid the torsion of the split conductor system when the conductor ice is falling off.

(4) When a single sub-conductor, a sub-conductor on the same side, and three sub-conductors are deiced simultaneously, the vertical jump height of the sub-conductor

on the lower side of the split conductor system is larger than that of the sub-conductor on the upper side. At the same time, there is a large lateral swing between the sub-conductors, resulting in torsion during deicing of the split conductor system. The maximum torsion angle during deicing of the sub-conductor on the same side reaches 16.6°. During deicing, the sub-conductors are prone to collision, which increases the risk of conductor wear.

REFERENCES

[1] *Anti Icing and Thawing Technology and Its Application in Power Grid*, China Southern Power Grid Corporation, Beijing, China, 2010.

[2] X. Jiang, Z. Zhang, Q. Hu, J. Hu, and L. Shu, "Thinkings on the restrike of ice and snow disaster to the power grid," *High Voltage Eng.*, vol. 44, no. 2, pp. 463–469, 2018.

[3] W. Yong, M. Hong, and M. Site, "Summary of research on anti-ice, ice melting and de-icing of high voltage overhead transmission lines," *Power Syst. Protection Control*, vol. 48, no. 18, pp. 178–187, 2022.

[4] C. Yafeng, Y. Yishi, and W. Cheng, "De-icing techniques for ice-covered transmission lines: A review," *High Voltage Appliances*, vol. 52, no. 11, pp. 1–9, 2016.

[5] S. Fan, M. Bi, Y. Gong, and X. Zhang, "Influence of ice shape around transmission line on ice melting process under natural condition," *High Voltage App.*, vol. 55, no. 6, pp. 184–191, 2019.

[6] L. Richeng, P. Junwen, and L. Huajiao, "A living DC ice-melting approach for UHV&EHV transmission lines," *J. Central South Univ., Sci. Technol.*, vol. 47, no. 5, pp. 1551–1558, 2016.

[7] W. Zhangqi, Q. I. Lizhong, and W. Jian, "Experiments on the dynamic tension of an overheadconductor under the asynchronous ice shedding," *J. Vib. Shock*, vol. 35, no. 22, pp. 61–65, 2016.

[8] H. Xinbo, "Analysis on influence factors of ice-shedding unbalanced tension of transmission tower-line system," *China Electric Power*, vol. 50, no. 11, pp. 96–102, 2017.

[9] L. Hongnan and W. Yuyan, "Experimental study on dynamic effect of ice shedding on transmission line," *China Civil Eng. J.*, vol. 52, no. 5, pp. 35–46, 2019.

[10] K. Ji, X. Rui, L. Li, A. Leblond, and G. McClure, "A novel ice-shedding model for overhead power line conductors with the consideration of adhesive/cohesive forces," *Comput. Struct.*, vol. 157, pp. 153–164, Sep. 2015.

[11] A. Jamaleddine, G. McClure, J. Rousselet, and R. Beauchemin, "Simulation of ice-shedding on electrical transmission lines using ADINA," *Pergamon*, vol. 52, pp. 4–5, Jun. 1993.

[12] W. Chuan et al., "Research on ice jump height and transverse swing of ultra-high voltage large cross-section conductor," *Chin. J. Appl. Mech.*, vol. 37, no. 5, pp. 2013–2020 and 2321, 2020.

[13] W. Tianbao et al., "Dynamic model of deicing jump in transmission lines," *Chin. J. Appl. Mech.*, vol. 35, no. 1, pp. 134–140 and 233, 2018.

[14] Y. Zhitao et al., "Chain deicing vibration of ice-covered transmission line considering height difference," *J. Hunan Univ., Natural Sci. Ed.*, vol. 47, no. 3, pp. 115–121, 2020.

[15] S. Gao, C. Zeng, L. Zhou, X. Liu, and B. Gao, "Numerical analysis of the dynamic effects of wine-cup shape power transmission tower-line system under ice-shedding," *Structures*, vol. 24, pp. 1–12, Apr. 2020.

[16] D. Yongxing et al., "Dynamic response of dissynchronous deicing of split conductor," *J. North China Electr. Power Univ., Natural Sci. Ed.*, vol. 45, no. 1, pp. 86–91 and 100, 2018.

[17] G. Huang, B. Yan, N. Wen, C. Wu, and Q. Li, "Study on jump height of transmission lines after ice-shedding by reduced-scale modeling test," *Cold Regions Sci. Technol.*, vol. 165, Sep. 2019, Art. no. 102781.

[18] H. Junke et al., "Dynamic response analysis of deicing jump of EHV/UHV multi circuit transmission lines on the same tower," *Power Grid Technol.*, vol. 36, no. 9, pp. 61–67, 2012.

[19] J. Xingliang et al., "Study on DC deicing and deicing process of conductor under natural conditions," *Power Grid Technol.*, vol. 37, no. 9, pp. 2626–2631, 2013.

[20] *Technical Specification for Design of DC Ice Melting System*, China Electr. Power Planning Eng. Inst., Beijing, China, 2006.

[21] L. Li et al., "Realization and application of parametric finite element method for deicing of transmission lines," *J. Huazhong Univ. Sci. Technol., Natural Sci. Ed.*, vol. 44, no. 4, pp. 68–73, 2016.

[22] S. Guohui et al., "Applicability analysis of finite element simulation method for wire icing deicing," *Eng. Mech.*, vol. 28, no. 10, pp. 9–15 and 40, 2011.

[23] X. Meng, L. Wang, L. Hou, G. Fu, B. Sun, M. MacAlpine, W. Hu, and Y. Chen, "Dynamic characteristic of ice-shedding on UHV overhead transmission lines," *Cold Regions Sci. Technol.*, vol. 66, no. 1, pp. 44–52, Apr. 2011.

[24] W. Nan et al., "Prediction model of conductor deicing jump height based on BP neural network," *J. Vib. Shock*, vol. 40, no. 1, pp. 199–204, 2021.

[25] Z. Diansheng, "Design Manual of high voltage transmission lines for power engineering," China Guodian Corp., Northeast Elect. Power Des. Inst., Beijing, China, Tech. Rep., 2003.

[26] B. Yan, K. Chen, Y. Guo, M. Liang, and Q. Yuan, "Numerical simulation study on jump height of iced transmission lines after ice shedding," *IEEE Trans. Power Del.*, vol. 28, no. 1, pp. 216–225, Jan. 2013.

[27] M. Suimin and K. Wei, "Tang Bo Overhead transmission line design," China Electr. Power Press, Beijing, China, Tech. Rep., 2015.

[28] C. Yong, H. Wei, W. Liming, and H. Lei, "Research on ice-shedding characteristic of icing conductor," *Proc. CSEE*, vol. 29, no. 28, pp. 115–121, 2009.

[29] J. Xingliang, S. Fan, J. Hu, Z. Zhang, and C. Sun, "Analysis of critical ice-melting current for short-circuit DC transmission line," *Proc. CSEE*, vol. 30, no. 1, pp. 111–116, 2010.
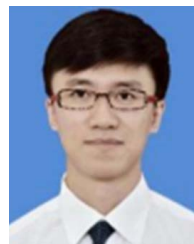
ZHU HE (Fellow, IEEE) received the Ph.D. degree. He is currently the Vice President of the Graduate School, Northeast Electric Power University. He is also a Visiting Scholar at Ottawa University, Canada, spring seedling talents for scientific research in colleges and universities in Jilin Province, outstanding young backbone teacher at Northeast Electric Power University and a Professor, mainly engaged in the research on operation and maintenance characteristics of UHV power grid under complex environment. He used to be the Deputy Director, the Dean, and the Vice President with the School of Architectural Engineering, Northeast Electric Power University. He is a master's tutor and famous teaching teacher of Northeast Electric Power University. He is a Senior Member of the China Society of Electrical Engineering and a member of the China Society of Degree and Graduate Education, the China Society of Mechanics, and the China Society of Renewable Energy.

TANG WENPENG received the master's degree. He is mainly engaged in research on transmission line operation and maintenance.

ZHANG RENQI received the bachelor's degree. He is currently a Senior Engineer. He is mainly engaged in the development of sleeve-type continuous sections of high-voltage conductor.

WANG WEIQI received the master's degree. He is mainly engaged in research on transmission line operation and maintenance.

LIAO HANLIANG received the master's degree. He is mainly engaged in research on transmission line operation and maintenance.

● ● ●